International Journal of Engineering and Advanced Technology Studies
Vol.7 No.1, pp.1-16, June 2019
Published by European Centre for Research Training and Development UK (www.eajournals.org)

A Single-Stage Three-Phase Boost Inverter for Grid-Connected Applications

Osama M. Salem[1*], Dina S.M. Osheba[2], Haitham Z. Azazi[2], and Azza E. Lashine[2]
[1]Assistant Researcher, Mechanical & Electrical Research Institute (31512), NWRC, Egypt.
[2]Electrical Engineering Dept., Faculty of Engineering, Menoufia University, Shebin El-kom, Egypt.

ABSTRACT: *Environmental pollution and economic issues are major problems that results in ascending increase of renewable sources such as solar energy. In order to utilize the current infrastructure of the grid for power transmission and distribution, grid-connected DC-to-AC inverters are needed. However, previously introduced inverters has a two power stage structure or a cascaded structure that increase the power losses and the complexity of the circuit. A new three-phase boost type grid connected inverter, which can be controlled by a new control methodology is proposed in this paper. The proposed inverter has only a single power stage converting DC power to AC power by injecting three sinusoidal currents into grid, which greatly reduces power losses and the complexity of the circuit. Also the proposed inverter can deliver active power from photovoltaic (PV) to the grid while continuously tracking maximum power point (MPP). This topology has several desirable features like simple circuitry, good stability and fast dynamic response. Operation principle, theoretical analysis and design of the proposed topology are discussed. Simulation results performed in MATLAB/SIMULINK software show the effectiveness of the proposed inverter topology.*

KEYWORDS: Three-phase, single-stage, boost inverters

INTRODUCTION

In recent years, PV systems have been widely used as an alternative power supply from natural energy. In such system, the PV inverter is required for interconnecting the grid and the PV system. In particular, the PV inverter is strongly required to achieve high efficiency [1-5]. The PV inverter is composed of a boost converter and an inverter. The boost converter is used to control the DC-link voltage, whereas the inverter converts the DC power to AC power. That is called Conventional PV systems or two-stage

Print ISSN: 2053-5783(Print), Online ISSN: 2053-5791(online)

systems, In those Conventional PV systems, a high-voltage DC-link capacitor is required with a large capacitance, which absorbs a power fluctuation caused by grid that increase the volume of the PV systems. Besides, the output voltage of PV modules is not high enough, that added a DC-DC boost converter that complicated the system [6]. Although these two stage systems are simple, they suffer from low efficiency, less reliability, more losses, and high cost [7]. On the other hand, the single-stage systems have been proposed in order to unify the DC-DC boost converter and the inverter. They are more reliable than multi-stage systems and offer higher efficiency. Furthermore, they have lower component than two stage systems that reduce the number of the switching devices, consequently increase the system power density [8-12].

As the generated power of the PV system depends heavily on the weather conditions and the solar radiation, the control of maximum power point tracking (MPPT) for the solar array is essential in a PV system. A large number of MPPT methods have been developed. Of these methods are perturb and observe (P&O), incremental conductance (IC), fractional short circuit current, fractional open circuit voltage, fuzzy logic based MPPT, and neural network based MPPT, Sweep MPPT method etc.. Although theses MPPTs methods are simple to implement, they have drawbacks such as power loss, oscillatory around MPP, and grid harmonics generated [13-17].

This paper proposes a topology of three-phase boost inverter connected with the grid. The proposed inverter has only a single power stage, converting DC power to AC power by injecting three sinusoidal currents into grid, which greatly reduces power losses and the complexity of the circuit. A new control circuit methodology is proposed. The proposed inverter is supplied from PV system that could feed the grid by electrical power with low harmonics produced while continuously tracking maximum power point (MPP). The proposed inverter topology and principle of operation will be explained. Also the state equations and the operation modes that describe the proposed topology are defined, then the waveforms of voltage, current and their harmonics spectrum are discussed and verified in detail. Finally simulation results performed in MATLAB/SIMULINK software shows the effectiveness of the proposed inverter when tied with the grid.

Print ISSN: 2053-5783(Print), Online ISSN: 2053-5791(online)

THE DESCRIPTION OF POWER TOPOLOGY PROPOSED

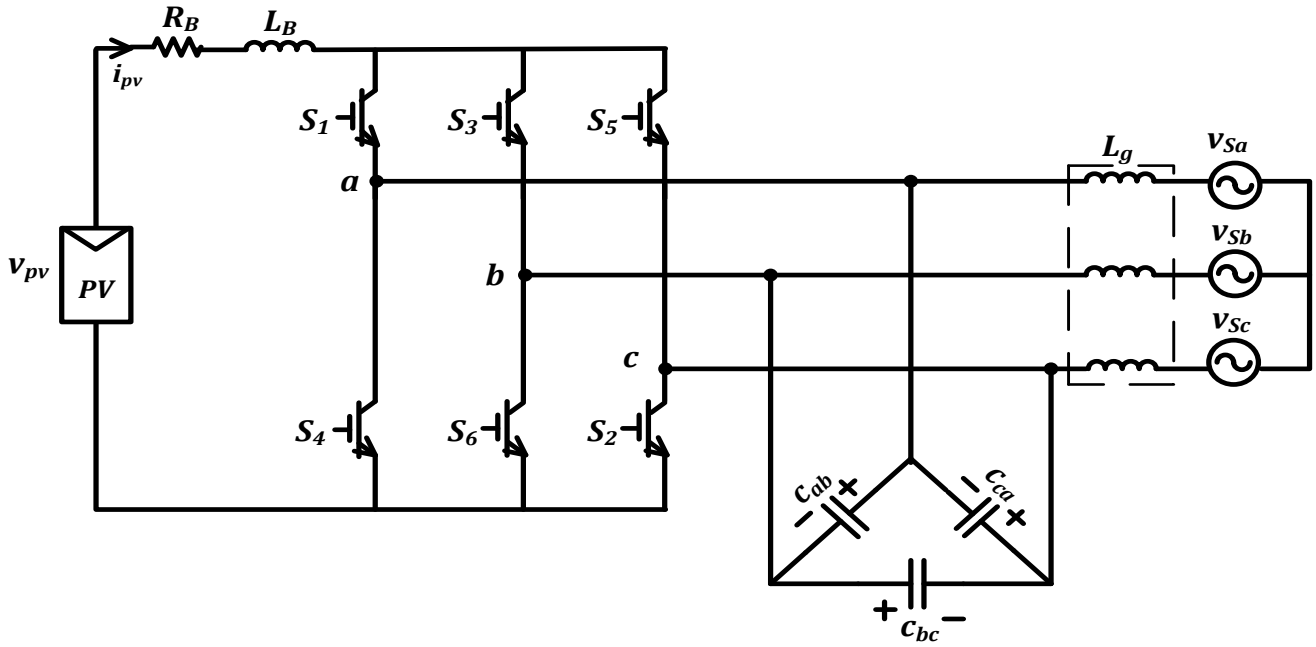

Fig. 1 The proposed boost inverter connected with the grid.

The circuit diagram of a grid-connected three-phase single-stage boost inverter is presented in Fig. 1. In this figure, v_{pv} is provided from the PV source, $L_B, and\ R_B$ is the boost inductor and its resistance, Delta connection capacitors represented by $C_{ab}, C_{bc}, and\ C_{ca}$. As can be seen in this figure, the boost inverter is connected to the grid $v_{sa}, v_{sb}, and\ v_{sc}$ through a grid interconnecting inductor L_g, , which is required for power flow control as well as filtering the injected current to the grid. Finally six power switches $S_1, S_2, S_3, S_4, S_5, and\ S_6$ to regulate the power delivered to the grid.

MODES OF OPERATIONS FOR THE TOPOLOGY PROPOSED

This section briefly describes the modes of operations for each switching state. There are six switching states defined by (ab, ac, bc, ba, ca, and cb) to generate three phase sinusoidal voltages. Each switching state has two modes, namely charging and discharging state. During the charging times the magnetic energy in L_B and the dc- current increased, while during the discharging time intervals, this current is injected to the output circuit.

Print ISSN: 2053-5783(Print), Online ISSN: 2053-5791(online)

A. At switching state (ab)

Mode 1: During this mode, only the switches S_1 and S_4 are closed, energy is stored in the inductor L_B and inductor current increased. The energy stored in the delta connection capacitor C_{ab}, C_{bc}, and C_{ca} is going to the grid. Equivalent circuit during this mode as shown in Fig. 2 (a). Equations could be written as (assuming ideal switches):

$$v_{ab} = v_{sa} - v_{sb} \quad (1)$$

$$v_{bc} = v_{sb} - v_{sa} \quad (2)$$

$$v_{ca} = v_{sc} - v_{sa} \quad (3)$$

$$v_{pv} = i_{pv} R_B + L_B \frac{di_{pv}}{dt} \quad (4)$$

Mode 2: During this mode, only the switches S_1 and S_6 are closed, the energy in the inductor L_B is transferred to the grid and capacitors C_{ab}, C_{bc}, and C_{ca}, and the voltage across the inductor L_B is reversed. The equivalent circuit during this mode is shown as in Fig. 2 (b). Equation could be written as (assuming ideal switches):

$$v_{pv} = i_{pv} R_B + L_B \frac{di_{pv}}{dt} + v_{ab} \quad (5)$$

$$v_{ab} = v_{sa} - v_{sb} \quad (6)$$

$$v_{bc} = v_{sb} - v_{sc} \quad (7)$$

$$v_{ca} = v_{sc} - v_{sa} \quad (8)$$

$$i_a + i_b + i_c = 0 \quad (9)$$

Print ISSN: 2053-5783(Print), Online ISSN: 2053-5791(online)

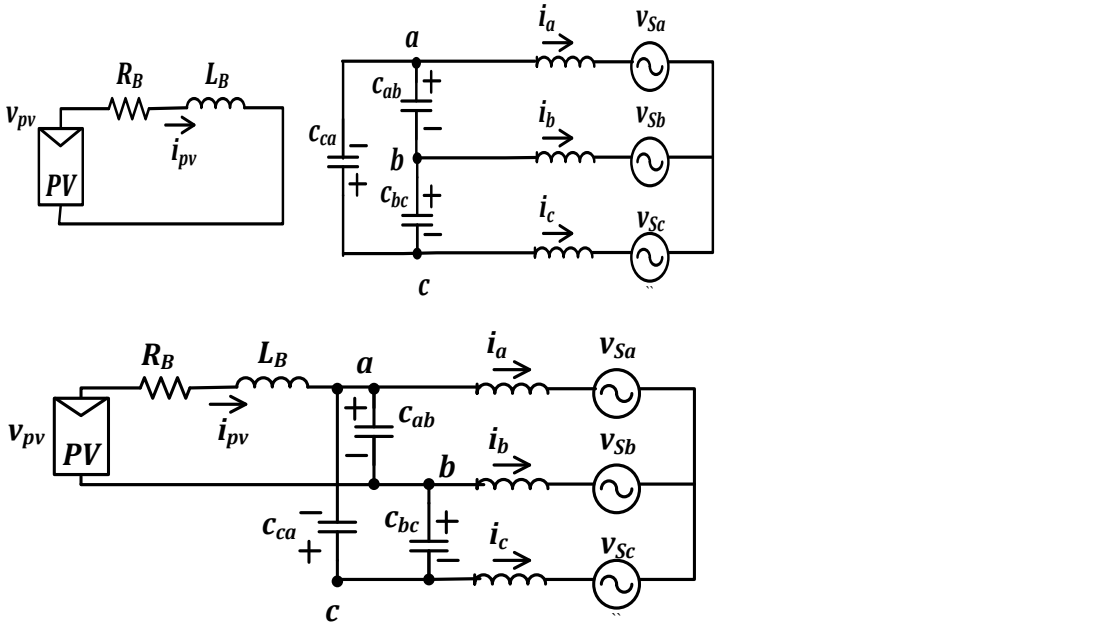

(a) (b)

Fig. 2; (a) Equivalent circuit during Mode 1, and (b) Equivalent circuit during Mode 2.

B. At Switching state (ac)

Mode 3: Similarly as in mode 1, when switches S_1 and S_4 are closed, energy is stored in the inductor L_B and inductor current increased. The energy stored in the delta connection capacitor C_{ab}, C_{bc}, and C_{ca} is going to the grid. This mode equations are the same of mode 1. Equivalent circuit during this mode as shown in Fig. 3 (a).

Mode 4: The same sequence of mode 2 is done as when switches S_1 and S_2 are closed, the energy in the inductor L_B is transferred to the grid and capacitors C_{ab}, C_{bc}, and C_{ca}, and the voltage across the inductor L_B is reversed. The equivalent circuit during this mode is shown as in Fig. 3 (b). Equation could be written as (assuming ideal switches):

$$v_{pv} = i_{pv} R_B + L_B \frac{di_{pv}}{dt} - v_{ac} \quad (10)$$

$$v_{ac} = -v_{ab} - v_{bc} \quad (11)$$

$$v_{ab} = v_{sa} - v_{sb} \quad (12)$$

$$v_{bc} = v_{sb} - v_{sc} \quad (13)$$

$$v_{ac} = v_{sc} - v_{sa} \quad (14)$$

$$i_a + i_b + i_c = 0 \quad (15)$$

Print ISSN: 2053-5783(Print), Online ISSN: 2053-5791(online)

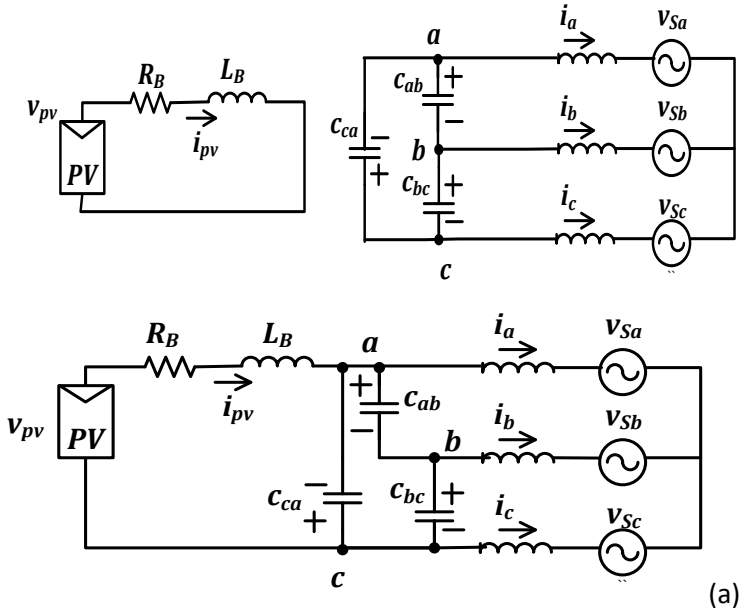

Fig. 3; (a) Equivalent circuit during Mode 3, and (b) Equivalent circuit during Mode 4.

C. At Switching state (bc)

Mode 5 (S_3 and S_6 are closed): Similarly as in mode 1. Fig. 4 (a) shows the equivalent circuit during this mode.

Mode 6 (S_3 and S_2 are closed): The same sequence of mode 2 is done. Fig. 4 (b) shows the equivalent circuit during this mode. Equations could be written as:

$$v_{pv} = i_{pv} R_B + L_B \frac{di_{pv}}{dt} + v_{bc} \quad (16)$$

$$v_{bc} = -v_{ab} - v_{ca} \quad (17)$$

$$v_{ab} = v_{sa} - v_{sb} \quad (18)$$

$$v_{bc} = v_{sb} - v_{sc} \quad (19)$$

$$v_{ca} = v_{sc} - v_{sa} \quad (20)$$

$$i_a + i_b + i_c = 0 \quad (21)$$

Print ISSN: 2053-5783(Print), Online ISSN: 2053-5791(online)

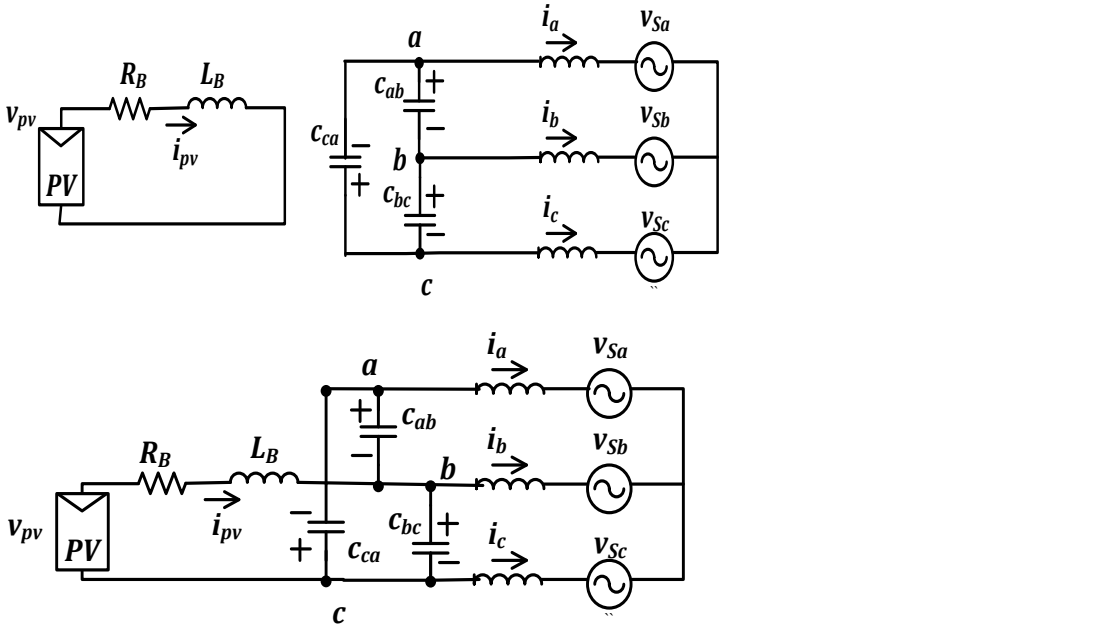

(a) (b)

Fig. 4; (a) Equivalent circuit during Mode 5, and (b) Equivalent circuit during Mode 6.

D. At Switching state (ba)

Mode 7 (S_3 and S_6 are closed): Similarly as in mode 1. Fig. 5 (a) shows the equivalent circuit during this mode.

Mode 8 (S_3 and S_4 are closed): The same sequence of mode 2 is done. Fig. 5 (b) shows the equivalent circuit during this mode. Equations could be written as:

$$v_{pv} = i_{pv} R_B + L_B \frac{di_{pv}}{dt} - v_{ba} \quad (22)$$

$$v_{ba} = v_{bc} + v_{ca} \quad (23)$$

$$v_{ba} = v_{sa} - v_{sb} \quad (24)$$

$$v_{bc} = v_{sb} - v_{sc} \quad (25)$$

$$v_{ca} = v_{sc} - v_{sa} \quad (26)$$

$$i_a + i_b + i_c = 0 \quad (27)$$

Print ISSN: 2053-5783(Print), Online ISSN: 2053-5791(online)

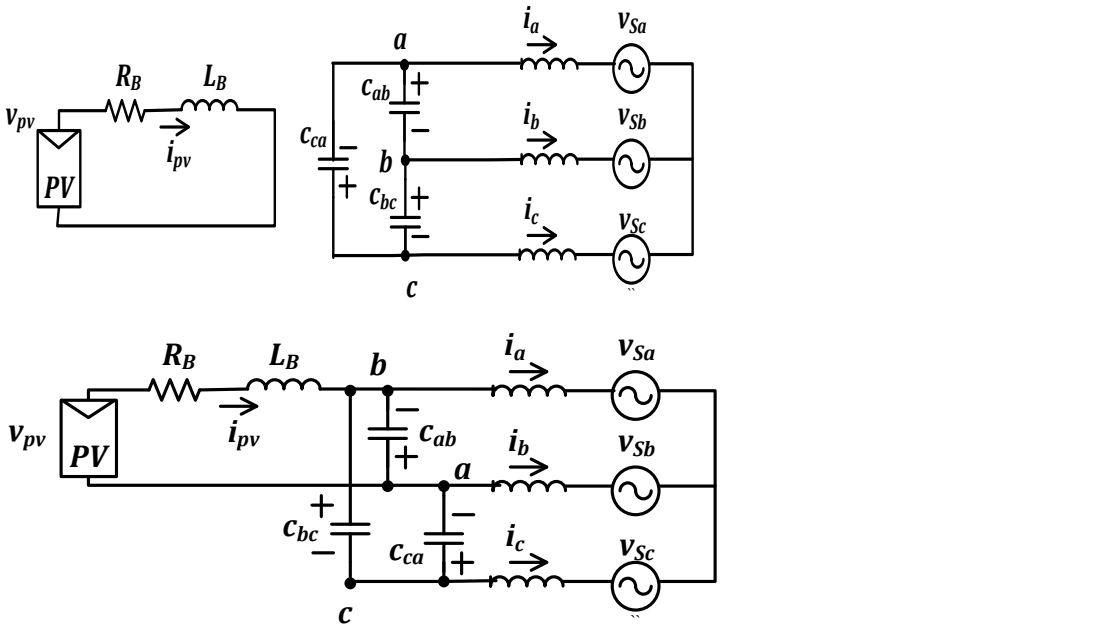

(a) (b)

Fig. 5; (a) Equivalent circuit during Mode 7, and (b) Equivalent circuit during Mode 8.

E. At Switching state (ca)

Mode 9 (S_5 and S_2 are closed): Similarly as in mode 1. Fig. 6 (a) shows the equivalent circuit during this mode.

Mode 10 (S_5 and S_4 are closed): The same sequence of mode 2 is done. Fig. 6 (b) shows the equivalent circuit during this mode. Equations could be written as:

$$v_{pv} = i_{pv} R_B + L_B \frac{di_{pv}}{dt} + v_{ca} \quad (28)$$

$$v_{ca} = -v_{ab} - v_{bc} \quad (29)$$

$$v_{ab} = v_{sa} - v_{sb} \quad (30)$$

$$v_{bc} = v_{sb} - v_{sc} \quad (31)$$

$$v_{ca} = v_{sc} - v_{sa} \quad (32)$$

$$i_a + i_b + i_c = 0 \quad (33)$$

Print ISSN: 2053-5783(Print), Online ISSN: 2053-5791(online)

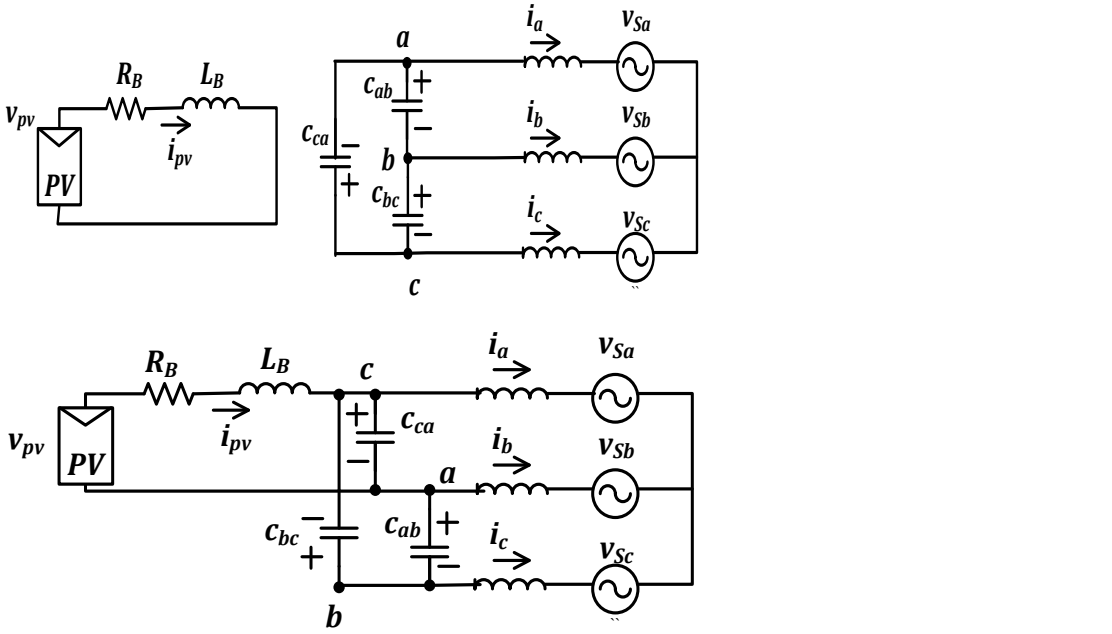

(a) (b)

Fig. 6; (a) Equivalent circuit during Mode 9, and (b) Equivalent circuit during Mode 10.

F. At Switching state (cb)

Mode 11 (S_5 and S_2 are closed): Similarly as in mode 1. The equivalent circuit during this mode is as shown in Fig. 7 (a).

Mode 12 (S_5 and S_6 are closed): The same sequence of mode 2 is done. Fig. 7 (b) shows the equivalent circuit during this mode. Equations could be written as:

$$v_{pv} = i_{pv} R_B + L_B \frac{di_{pv}}{dt} + v_{cb} \quad (34)$$

$$v_{cb} = v_{ab} + v_{ca} \quad (35)$$

$$v_{ab} = v_{sa} - v_{sb} \quad (36)$$

$$v_{cb} = v_{sb} - v_{sc} \quad (37)$$

$$v_{ca} = v_{sc} - v_{sa} \quad (38)$$

$$i_a + i_b + i_c = 0 \quad (39)$$

Print ISSN: 2053-5783(Print), Online ISSN: 2053-5791(online)

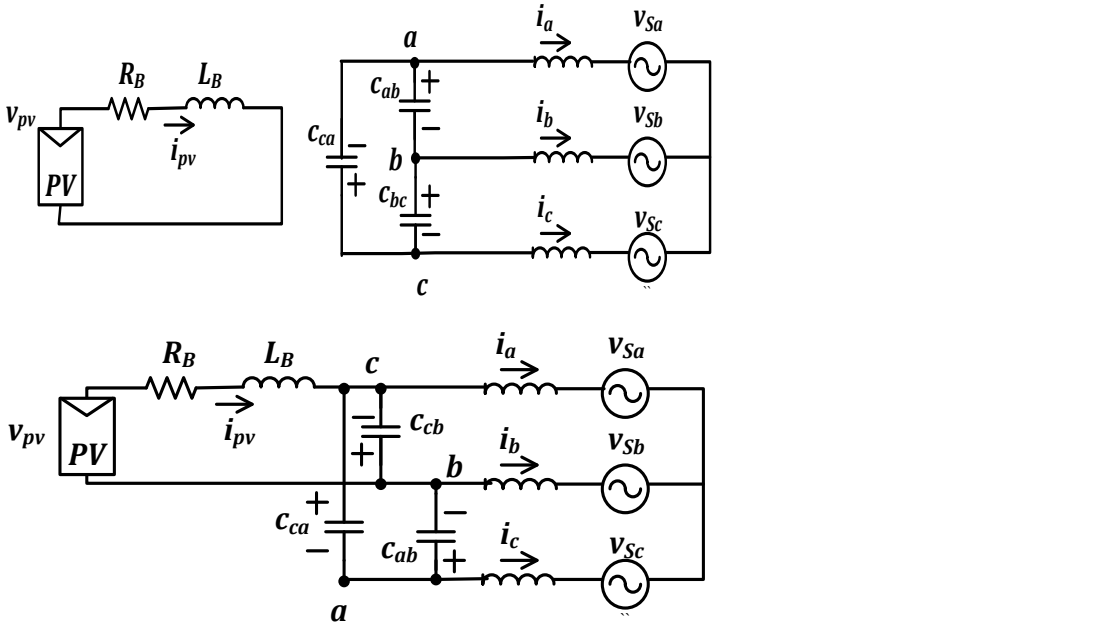

(a) (b)

Fig. 7; (a) Equivalent circuit during Mode 11, and (b) Equivalent circuit during Mode 12.

Where v_{ab} is the difference voltage between point (a) and point (b), v_{bc} is the difference voltage between point (b) and point (c), v_{ca} is the difference voltage between point (c) and point (a), i_a, i_b, i_c are the three phase grid currents, and i_{pv} is the source PV current.

PROPOSED CONTROL STRATEGY

Because of the nonlinear characteristic of PV arrays, maximum power cannot be achieved by directly connecting the PV arrays. As mentioned before, there are a lot of methods of MPPT used. Due to their problems encountered, such as power loss, harmonics and problems due to on line measurements. A new MPPT control method is introduced with the proposed inverter control strategy. This new MPPT control method got the voltage at maximum power point v_{mpp} easily, that is achieved by determining a reference voltage refers to v_{mpp} and put it as a reference signal as shown in Fig. 8. The voltage of the PV source v_{pv} is then compared with the reference voltage v_{mpp} and is going through PI controller, the output of the PI controller is multiply with the three phase grid voltages generating i_{mpp} for each phase. This output of i_{mpp} for each phase is confront with the PV current i_{pv}, then the outcome is passed through a hysteresis controller. The result of that hysteresis controller is compared with the logic control signals through the mode selector block producing the gate pulses to the power switches. These

Print ISSN: 2053-5783(Print), Online ISSN: 2053-5791(online)

logic control signals resulted by the help of logic AND&OR gates that compare the three phase grid voltages to detect each switching state that are the higher value of each phase of the grid voltages.

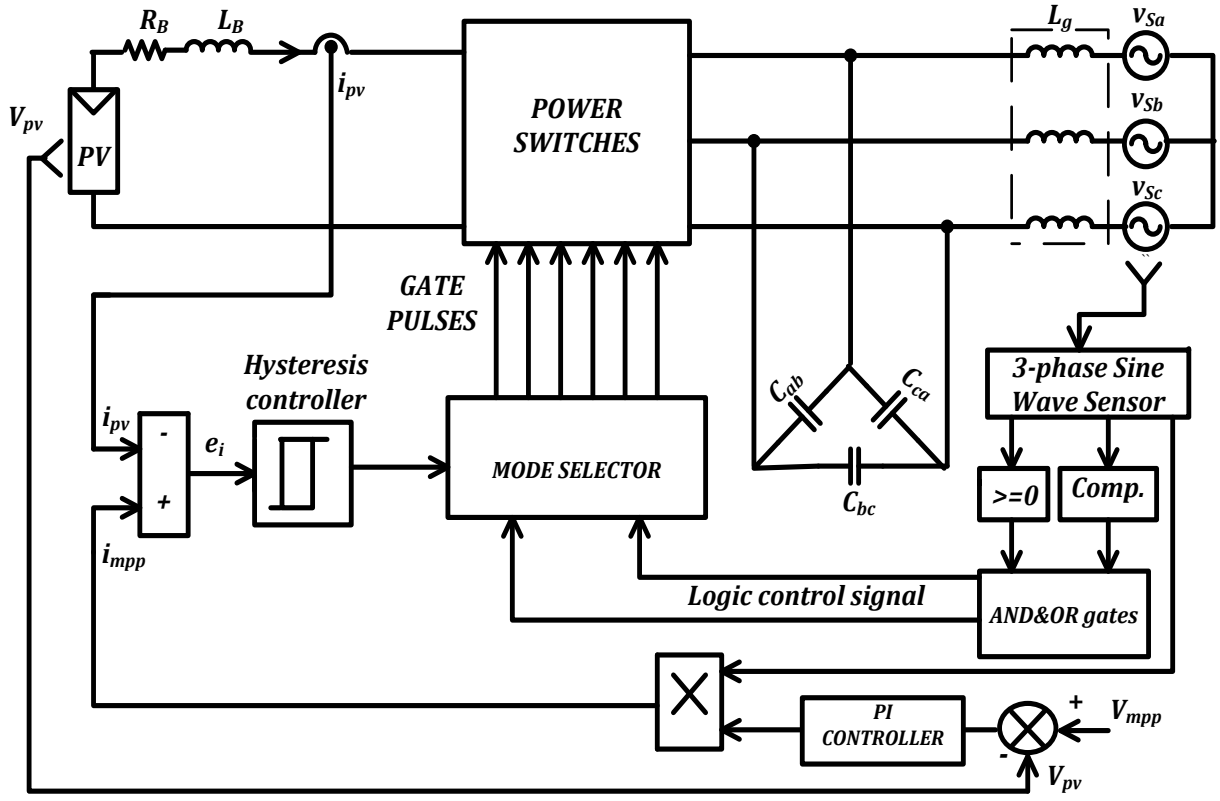

Fig. 8 The proposed control strategy.

SIMULATION RESULTS

In order to validate the theoretical analysis, the three-phase boost inverter with the proposed control strategy has been built and simulated. Simulation is carried out to determine the characteristics of the proposed circuit. The output of the inverter is connected to a 50 Hz sinusoidal voltage for grid connected operation. The simulations are conducted in MATLAB/SIMULNK software, with parameters listed in Table 1. The PV voltage is determined by connecting three module in series that its electrical characteristics is mentioned as Table 2 for each module.

Print ISSN: 2053-5783(Print), Online ISSN: 2053-5791(online)

Table 1, Parameters of the boost inverter.

Item	Symbol	Value
Coil Resistance	R_B	0.5 Ω
Coil Inductance	L_B	20 mH
Capacitor Capacitance	$C_{\text{ab}}, C_{\text{bc}}, C_{\text{ca}}$	50 µF
AC grid voltage (RMS)	v_{sa}, v_{sb}, v_{sc}	220 V,50 HZ
Grid Inductance	L_g	10 mH

Table 2, Electrical characteristics of the PV module at standard test conditions.

Electrical Characteristics	*Value*
$I_{sc}\ (A)$	8
$V_{oc}\ (V)$	37.39
$I_{mp}\ (A)$	7.19
$V_{mp}\ (V)$	27.8
$P_{max}\ (W)$	200

By applying a step change in radiation by decreasing it from radiation Ir =1000 to Ir =900 w/m^2, and by using the new technique of MPPT that determine the voltage at MPP as a reference voltage by experimental measurements for different radiations levels. As could be seen from table 2 that each module has v_{mpp} =27.8 volt at Ir =1000 w/m^2. From the experimental results and for any radiation levels if v_{mpp} is set equal to 26.5 volt, the loss in p_{mpp} (power at v_{mpp}) is approx. nonexistent. That is evident from simulation results as shown in Fig. 9.

Fig. 9 (b, and c) illustrate that with the insolation is changed from Ir =1000 to Ir =900 w/m^2. The injected PV output power and current are nearly close to both the maximum power p_{mp} and maximum current i_{mp} and decreased with insolation decreased. Fig. 9 (d) shows the PV output voltage is constant at the value of 79.5 volt, that is the product of 3 module* 26.5 volt, reference value for each module. That ensure the availability of control methodology proposed.

Fig. 9 (e, and g) ensures that the new topology and its control structure are capable of boosting the input DC voltage to the required AC level with almost sinusoidal characteristics, also with the variation of insulation from Ir =1000 to Ir =900 w/m^2 the proposed control strategy ensures that the PV system proposed supply the grid by approx. constant symmetrical output voltages and currents having a pure sine wave with very low harmonics component as shown in Fig. 9 (f, and h). As it could be seen from the figures that THD for the injected voltages is 1.6% and 2.1% for the injected currents.

Print ISSN: 2053-5783(Print), Online ISSN: 2053-5791(online)

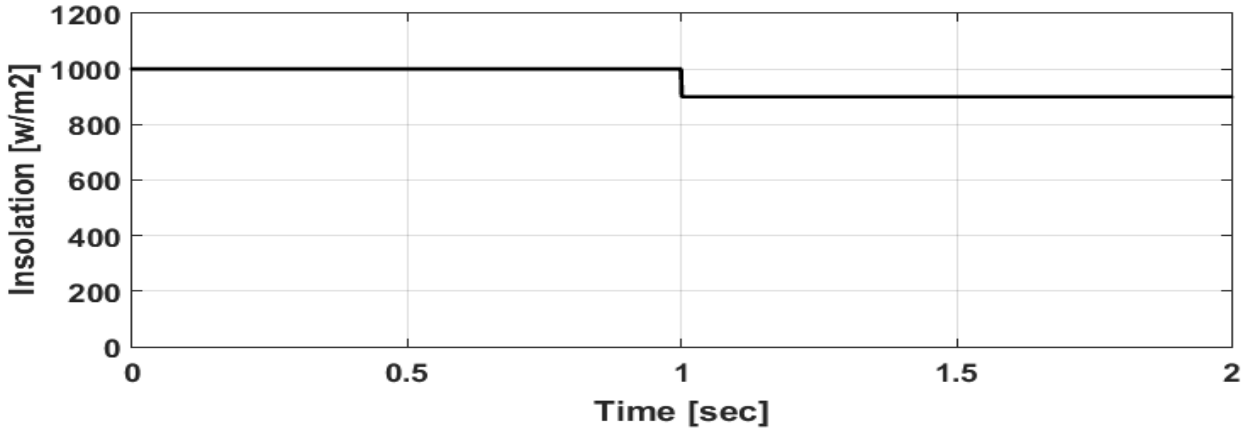

(a)

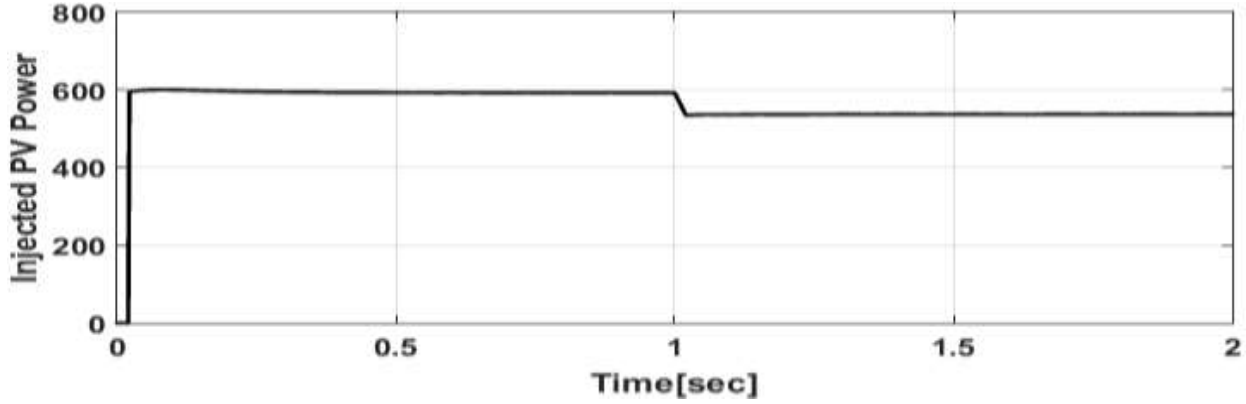

(b)

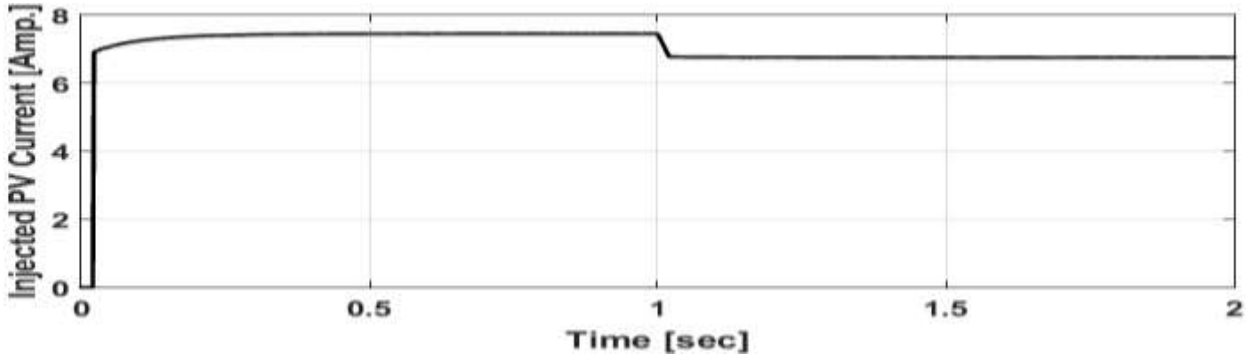

(c)

Print ISSN: 2053-5783(Print), Online ISSN: 2053-5791(online)

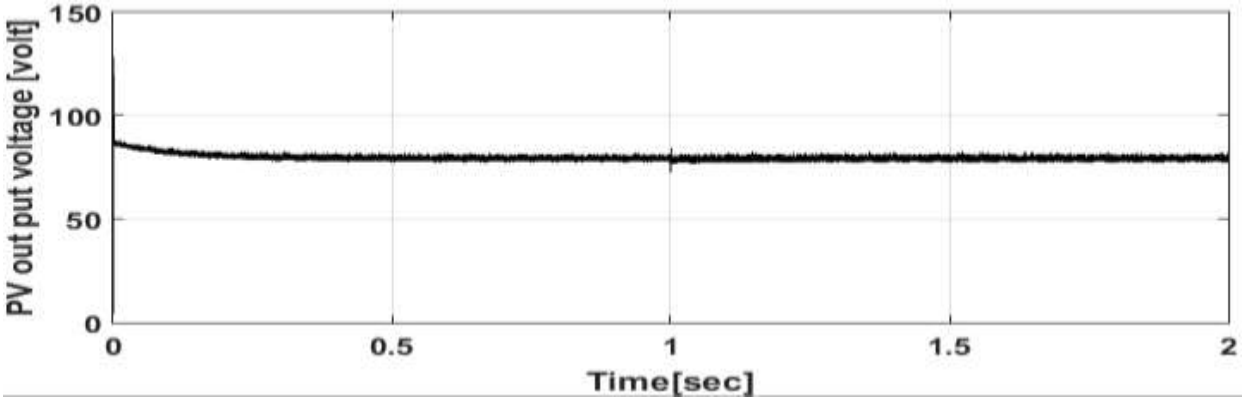

(d)

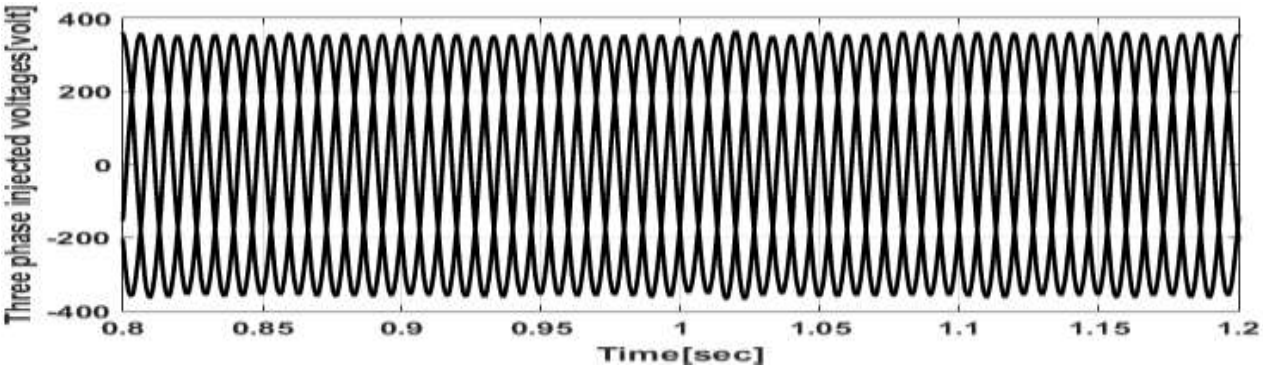

(e)

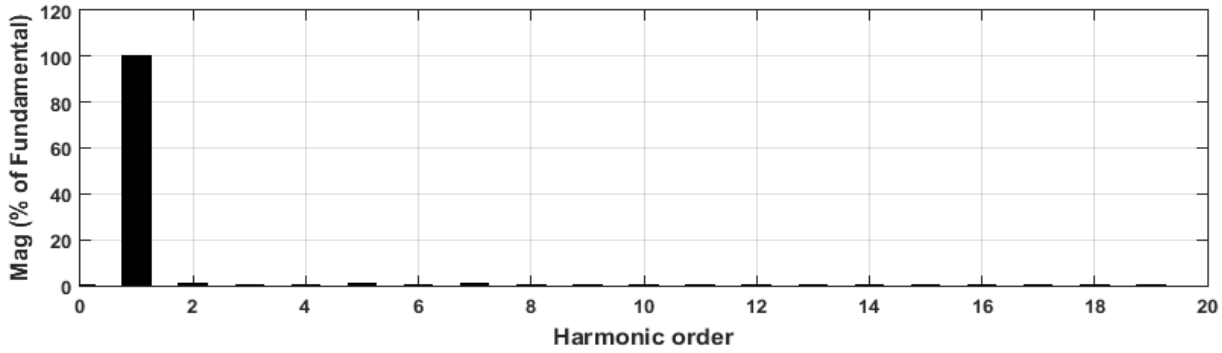

(f)

Print ISSN: 2053-5783(Print), Online ISSN: 2053-5791(online)

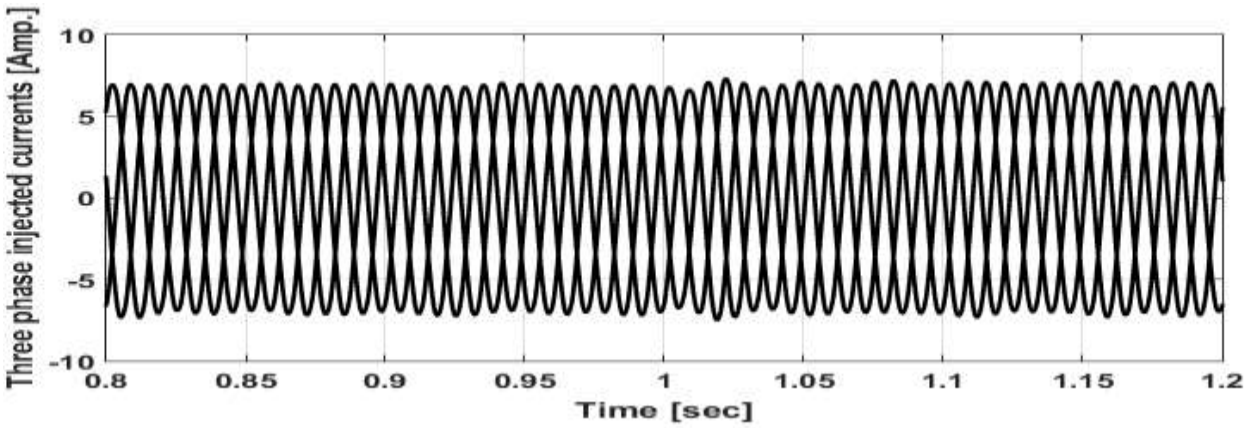

(g)

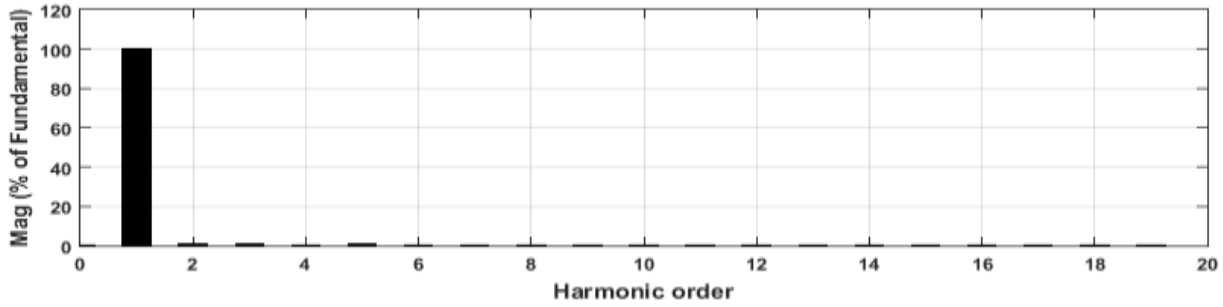

(h)

Fig. 9 Variation of PV power, PV current, and PV voltage, injected voltages, and currents with their harmonics using MPPT proposed method with a step change in radiation from Ir =1000 to Ir =900 w/m^2.

CONCLUSION

In this paper, a three-phase boost type grid-connected inverter is proposed. A new control methodology is proposed also for that type of grid-connected inverter. It has only a single power stage which greatly reduces power losses and the complexity of the circuit. The proposed inverter can convert DC power into AC power by injecting three sinusoidal currents to the grid with low total harmonic distortions (1.6% for injected voltages and 2.1 for injected currents). The proposed topology has several desirable features like simple circuitry, good stability and fast dynamic response. The proposed circuit topology offers a good harmonic profile and regulation of the injected voltages and currents waveforms when applying the MPPT control algorithm, as evidenced from the simulation studies when tied with the grid.

Print ISSN: 2053-5783(Print), Online ISSN: 2053-5791(online)

REFERENCES

[1]S. Saridakis, E. Koutroulis, F. Blaabjerg : "Optimization of SiC-Based H5 and Conergy-NPC Transformer less PV Inverters", IEEE Journal of Emerging and Selected Topics in Power Electronics, Vol. 3, No. 2, pp. 555-567, 2015.
[2] Y. Zhou, H. Li, H. Li : "A Single-Phase PV Quasi-Z-Source Inverter With Reduced Capacitance Using Modified Modulation and Double-Frequency Ripple Suppression Control", IEEE Transactions on Power Electronics, Vol. 31, No. 3, pp. 2166-2173, 2016.
[3] R. Chattopadhyay, S. Bhattacharya, N. C. Foureaux, I. A. Pires, H. de Paula, L. Moraes, P. C. Cortizio, S. M. Silva, B. C. Fil-ho, Jose A. de S. Brito,"Low-Voltage PV Power Integration into Medium Voltage Grid Using High-Voltage SiC Devices", IEE J Journal of Industry Applications, vol.4, no.6, pp.767-775, 2015.
[4] S. Saridakis, E. Koutroulis, F. Blaabjerg : "Optimization of SiC-Based H5 and Con-ergy-NPC Transformer less PV Inverters", IEEE Journal of Emerging and Selected Topics in Power Electronics, vol. 3, no. 2, pp. 555-567, 2015.
[5] S. Yamaguchi, T. Shimizu,"Single-phase Power Conditioner with a Buck-boost-type Power Decoupling Circuit", IEEJ J. Industry Applications, vol.5, no.3, pp.191-198, 2016.
[6] S. S. Nag and S. Mishra, "A coupled inductor based high boost inverter with sub-unity turns-Ratio range," IEEE Trans. Power Electron., vol. 31, no. 2, pp. 7534-7543,2016.
[7] Y. Zhou and W. Huang, "Single-Stage Boost Inverter with Coupled Inductor," IEEE Trans. Power Electron. vol. 27, no. 4, pp. 1885–1893, April 2012.
[8] M. Jang, V. G. Agelidis : "A Minimum Power-Processing-Stage FuelCell Energy System Based on a Boost-Inverter with a Bidirectional Backup Battery Storage", IEEE Trans. on Power Electronics, Vol. 26, No. 5, pp. 1568-1577 (2011).
[9] Y. Zhou and W. Huang, "Single-stage boost inverter with coupled inductor," IEEE Trans. Power Electron., vol. 27, no. 4, pp. 1885-1893, 2012.
[10] A. Darwish, A. M. Massoud, D. Holliday, S. Ahmed and B. W.Williams, "Single-stage three-phase differential-mode buck-boost inverters with continuous input current for PV applications," IEEE Trans. Power Electron., vol. 31, no. 12, pp. 8218-8236,2016.
[11] Y. Zhou, W. Huang, P. Zhao and J. Zhao, "Coupled-inductor single stage boost inverter for grid-connected photovoltaic system," IET Power Electron., vol. 7, no. 2, pp. 259-270, 2014.
[12] Y. Tang, Y. Bai, J. Kan, F. Xu : "Improved Dual Boost Inverter With Half Cycle Modulation", IEEE Transactions on Power Electronics, vol. 32, no. 10, pp. 7543-7552, (2017).
[13]C. Manickam, G. R. Raman, G. P.Raman, S. I. Ganesan, C. Nagamani, "A Hybrid Algorithm for Tracking of GMPP Based on P&O and PSO With Reduced Power Oscillation in String Inverters", IEEE Trans. Ind. Electron., vol. 63, pp. 6097–6106, 2016.
[14]M. M. Shebani, T. Iqbal, J. E. Quaicoe," Comparing bisection numerical algorithm with fractional short circuit current and open circuit voltage methods for MPPT photovoltaic systems", In Proceedings of the 2016 IEEE Electrical Power and Energy Conference (EPEC), pp. 1–5, 2016.
[15]H. Ahmed, A. F. Murtaza, A. Noman, K. E. Addowesh, and M. chiaberge,''An intelligent control strategy of fractional short circuit current maximum power point tracking technique for photovoltaic application", J. Renw. Sustain. Energy, 2015.
[16]K. M. Tsang, W. L. Chan," Maximum power point tracking for PV systems under partial shading conditions using current sweeping", J. Energy Conv. Management , vol. 93, pp. 249-258, 2015.
[17]M. Rizwan, M. Jamil, S. Kirmani, and D. P. Kothari," Fuzzy logic based modelling and estimation of global solar energy using meteorological parameters", J. Energy, vol.70, pp.685-691, 2014.

Print ISSN: 2053-5783(Print), Online ISSN: 2053-5791(online)